SPR Biosensing in Crude Serum Using Ultralow Fouling Binary Patterned Peptide SAM

ARTICLE *in* ANALYTICAL CHEMISTRY · MARCH 2010

Impact Factor: 5.64 · DOI: 10.1021/ac100035s · Source: PubMed

3 AUTHORS, INCLUDING:

Joelle N Pelletier
Université de Montréal
77 PUBLICATIONS **1,684** CITATIONS
SEE PROFILE

Jean-Francois Masson
Université de Montréal
90 PUBLICATIONS **1,266** CITATIONS
SEE PROFILE

Anal. Chem. **2010,** *82,* 3699–3706

SPR Biosensing in Crude Serum Using Ultralow Fouling Binary Patterned Peptide SAM

Olivier R. Bolduc,[†] Joelle N. Pelletier,[†,‡] and Jean-François Masson*[,†,§,∥]

Département de Chimie, PROTEO Network for Protein Structure, Function and Engineering, Centre for Self-Assembled Chemical Structures (CSACS), and Centre for Biorecognition and Biosensors (CBB), Université de Montréal, C. P. 6128 Succ. Centre-Ville, Montréal, Quebec, Canada, H3C 3J7

Near-zero fouling monolayers based on binary patterned peptides allow low nanomolar detection of the matrix metalloproteinase-3 (MMP-3) directly in crude bovine serum, without sample pretreatment, secondary antibody detection or signal amplification. The peptide 3-MPA-HHHDD-OH (3-MPA, 3-mercaptopropionic acid) was found optimal compared to other binary patterned peptides based on 3-MPA-A_x-B_y-OH, where $0 \leq x, y \leq 5$, and $x + y = 5$, and compared to PEG. In this study, amino acid A was His, Asp, Ser, or Leu, and amino acid B was His, Asp, or Ser. Zwitterionic peptides and other peptides exhibited excellent resistance to nonspecific adsorption. Binary patterned peptides were capped with 3-MPA on the *N*-terminus providing a monolayer with the C-terminus carboxylic acid available to subsequently immobilize antibodies. Thereby, an IgG biosensor demonstrated the efficiency of binary patterned peptides in SPR biosensing with a detection limit of 1−10 pM in PBS, similar to other optical or electrochemical techniques. This protocol was applied to establish a calibration curve for MMP-3, an analyte of clinical interest for many pathologies and a potential indicator of cancer. The LOD for MMP-3 was 0.14 nM in PBS, with a linearity of up to 50 nM. With the use of PBS calibration, MMP-3 was quantified at low nanomolar in undiluted bovine serum. The SPR response in serum was statistically the same as in PBS. A sensor exposed to blank serum exhibited negligible nonspecific adsorption. Hence, binary patterned peptides are suitable for biosensing directly in complex biological matrixes.

Surface plasmon resonance (SPR) has evolved into a useful bioanalytical tool to detect proteins, DNA, enzymes, and other biomolecules.[1] The excellent sensitivity of SPR for detecting proteins explains the increasing popularity of SPR. However, biomolecule detection in complex matrixes (such as cell lysate, serum, and blood) is greatly limited because of nonspecific interactions on SPR biosensors. Nonspecific proteins interact with the surface of biosensors creating a false positive response, hindering the detection of analytes in crude biological fluids. Thus, it is necessary to reduce nonspecific interactions to allow the use of biosensors for direct monitoring of biomolecules in biological fluids, eliminating the need of cleaning steps, signal amplification, labeling, or indirect detection of the analyte.

Immobilized molecular receptors on self-assembled monolayers are used to specifically detect biomolecules with SPR sensors.[2] Ideally, the monolayer should protect the SPR surface from nonspecific adsorption and provide an anchoring point for the molecular receptor to the SPR surface. Hence, extensive research in surface chemistry has been undertaken in the past decade to overcome nonspecific adsorption. In fact, the high sensitivity of SPR to protein adsorption also makes it an excellent tool to monitor nonspecific adsorption on self-assembled monolayers.[3] Dextran polymers have been extensively used in SPR biosensing, with mitigated results in complex biological fluids. The higher molecular weight dextrans, which are essential for the sensitive detection of analytes, fail to protect the SPR surface.[4,5] CM-Dextran exhibits nonspecific adsorption on the order of 859 ng/cm^2 in serum[5] (we replicated this result at 829 ± 46 ng/cm^2), significantly higher than PEG at 100 ng/cm^2 measured under identical experimental conditions.[6] Structure−property studies revealed that thiol monolayers with polar head groups were especially efficient in resisting nonspecific adsorption.[7−9] Among layers investigated in those studies, polyethyleneglycol (PEG), also known as polyethylene oxide (PEO), offered optimal performances in limiting nonspecific adsorption.[8] Numerous variants of PEG monolayers have been investigated for nonspecific

* To whom correspondence should be addressed. Tel: 1-514-343-7342. Fax: 1-514-343-7586. E-mail: jf.masson@umontreal.ca.

[†] Département de Chimie.

[‡] PROTEO Network for Protein Structure, Function and Engineering.

[§] Centre for Self-Assembled Chemical Structures (CSACS).

[∥] Centre for Biorecognition and Biosensors (CBB).

(1) Homola, J.; Yee, S. S.; Gauglitz, G. *Sens. Actuators, B* **1999**, *54*, 3–15.

(2) Wink, T.; vanZuilen, S. J.; Bult, A.; vanBennekom, W. P. *Analyst* **1997**, *122*, R43−R50.

(3) Mrksich, M.; Sigal, G. B.; Whitesides, G. M. *Langmuir* **1995**, *11*, 4383–4385.

(4) Frazier, R. A.; Matthijs, G.; Davies, M. C.; Roberts, C. J.; Schacht, E.; Tendler, S. J. B. *Biomaterials* **2000**, *21*, 957–966.

(5) Masson, J. F.; Battaglia, T. M.; Davidson, M. J.; Kim, Y. C.; Prakash, A. M. C.; Beaudoin, S.; Booksh, K. S. *Talanta* **2005**, *67*, 918–925.

(6) Bolduc, O. R.; Clouthier, C. M.; Pelletier, J. N.; Masson, J. F. *Anal. Chem.* **2009**, *81*, 6779–6788.

(7) Chapman, R. G.; Ostuni, E.; Yan, L.; Whitesides, G. M. *Langmuir* **2000**, *16*, 6927–6936.

(8) Ostuni, E.; Chapman, R. G.; Holmlin, R. E.; Takayama, S.; Whitesides, G. M. *Langmuir* **2001**, *17*, 5605–5620.

(9) Silin, V.; Weetall, H.; Vanderah, D. J. *J. Colloid Interface Sci.* **1997**, *185*, 94–103.

10.1021/ac100035s
Published on Web 03/30/2010

adsorption.[10−13] Although PEG monolayers have been used for detection of proteins in serum,[14] they exhibit limitations including nonzero fouling, oxidative damage, and the need for carboxylic acid functionalization of PEG to immobilize the molecular receptor.

Hybrid materials have been designed to improve on the properties of PEG. As examples, PEG copolymers of maleimide-PEG monolayers,[15,16] polypropylene sulfide-PEG,[17] and poly(l-lysine)-PEG[18] were all successful in resisting nonspecific adsorption. The later combines the properties of peptides with PEG. This approach was further developed by the group of Messersmith, who successfully developed a peptidomimetic polymer with ethylene glycol brushes.[19,20] This surface limited nonspecific adsorption from cells on a metallic surface. Similarly, a poly(aspartic acid) peptide with ethylene glycol (EG)-biotin brushes exhibited low nonspecific adsorption and could provide immobilization of molecules via biotin-streptavidin-modified EG and biotinylated antibodies.[21,22]

The idea of using peptide monolayers to minimize nonspecific adsorption of biological media to SPR surfaces is attractive. The varied physicochemical properties of the side chains provide prospects for tuning the surface properties, while the N-terminal amino acid is well suited to bind to a carboxy-terminated thiol, exposing the terminal carboxylic acid of the peptide to the solution for specific protein immobilization. To this end, we have previously studied the structure−property relationships of amino acid monolayers resistant to nonspecific adsorption.[23] This allowed selection of amino acids with optimal properties, small, polar, and ionic, in accordance with previous results obtained for organic monolayers.[8,9] Peptide monolayers were also demonstrated to reduce nonspecific adsorption to a level equivalent to PEG according to previous work, sufficient for biomolecule detection in complex matrixes such as crude cell lysate.[6,24] Ultralow fouling was recently reported based on zwitterionic monolayers,[25−27] allowing protein detection in blood plasma.[28] Peptide monolayers are synthetically simple to prepare and highly tunable with the broad range of natural and synthetic amino acids available. Hence, the capacity of zwitterionic and nonzwitterionic peptides in achieving ultralow fouling, immobilization of recognition biomolecules and low level detection of proteins in serum will be investigated.

Matrix metalloproteinase-3 (MMP-3) is an enzyme involved in important pathologies including atherosclerotic plaques,[29,30] circulatory malfunctions,[31,32] arthritis,[33] chronic liver diseases,[34] and different types of cancer.[33,35−43] MMP-3 is a proteinase involved in the degradation of the extracellular matrix; therefore, it potentially plays an important role in metastasis development during the early stage of invasive cancers.[39,40] In those and other pathologies, it has been shown that the serum concentration of MMP-3 is upregulated up to four times relative to its normal abundance.[29,35,38−40] Depending on the experimental conditions used for the recovery of the media containing MMP-3 and the analytical techniques used to quantify this analyte, the normal concentration of MMP-3 (for healthy subjects) in serum varies from 0.7[30] to 7 nM.[34,35] Unamplified SPR biosensing typically reaches a limit of detection (LOD) in the low nanomolar or picomolar range. Therefore, MMP-3 concentrations are within the range of detection by SPR. Although MMP-3 quantification alone could not be used to give a clear diagnostic for the pathologies listed before, it is a marker of great clinical importance. Because the variation in serum MMP-3 concentration in the above-mentioned diseases is modest, high-precision analytical detection is essential. Moreover, its low abundance in biological fluids makes it an ideal model for demonstrating the potential of binary patterned peptide SAMs for a direct detection assay in complex biological matrixes.

(10) Trmcic-Cvitas, J.; Hasan, E.; Ramstedt, M.; Li, X.; Cooper, M. A.; Abell, C.; Huck, W. T. S.; Gautrot, J. E. *Biomacromolecules* **2009**, *10*, 2885–2894.
(11) Uchida, K.; Hoshino, Y.; Tamura, A.; Yoshimoto, K.; Kojima, S.; Yamashita, K.; Yamanaka, I.; Otsuka, H.; Kataoka, K.; Nagasaki, Y. *Biointerphases* **2007**, *2*, 126–130.
(12) Uchida, K.; Otsuka, H.; Kaneko, M.; Kataoka, K.; Nagasaki, Y. *Anal. Chem.* **2005**, *77*, 1075–1080.
(13) Zareie, H. M.; Boyer, C.; Bulmus, V.; Nateghi, E.; Davis, T. P. *ACS Nano* **2008**, *2*, 757–765.
(14) Teramura, Y.; Iwata, H. *Anal. Biochem.* **2007**, *365*, 201–207.
(15) Lee, C. Y.; Gamble, L. J.; Grainger, D. W.; Castner, D. G. *Biointerphases* **2006**, *1*, 82–92.
(16) Lee, C. Y.; Nguyen, P. C. T.; Grainger, D. W.; Gamble, L. J.; Castner, D. G. *Anal. Chem.* **2007**, *79*, 4390–4400.
(17) Feller, L. M.; Cerritelli, S.; Textor, M.; Hubbell, J. A.; Tosatti, S. G. P. *Macromolecules* **2005**, *38*, 10503–10510.
(18) Tosatti, S.; Paul, S. M. D.; Askendal, A.; VandeVondele, S.; Hubbell, J. A.; Tengvall, P.; Textor, M. *Biomaterials* **2003**, *24*, 4949–4958.
(19) Statz, A. R.; Barron, A. E.; Messersmith, P. B. *Soft Matter* **2008**, *4*, 131–139.
(20) Statz, A. R.; Meagher, R. J.; Barron, A. E.; Messersmith, P. B. *J. Am. Chem. Soc.* **2005**, *127*, 7972–7973.
(21) Jeong, J. H.; Kim, B. Y.; Cho, S. H.; Kim, J. D. *J. Nonlinear Opt. Phys. Mater.* **2004**, *13*, 525–534.
(22) Jeong, J. H.; Kim, B. Y.; Lee, S. J.; Kim, J. D. *Chem. Phys. Lett.* **2006**, *421*, 373–377.
(23) Bolduc, O. R.; Masson, J. F. *Langmuir* **2008**, *24*, 12085–12091.
(24) Kyo, M.; Usui-Aoki, K.; Koga, H. *Anal. Chem.* **2005**, *77*, 7115–7121.
(25) Chen, S. F.; Cao, Z. Q.; Jiang, S. Y. *Biomaterials* **2009**, *30*, 5892–5896.
(26) Vaisocherova, H.; Yang, W.; Zhang, Z.; Cao, Z. Q.; Cheng, G.; Piliarik, M.; Homola, J.; Jiang, S. Y. *Anal. Chem.* **2008**, *80*, 7894–7901.
(27) Holmlin, R. E.; Chen, X. X.; Chapman, R. G.; Takayama, S.; Whitesides, G. M. *Langmuir* **2001**, *17*, 2841–2850.
(28) Vaisocherova, H.; Zhang, Z.; Yang, W.; Cao, Z. Q.; Cheng, G.; Taylor, A. D.; Piliarik, M.; Homola, J.; Jiang, S. Y. *Biosens. Bioelectron.* **2009**, *24*, 1924–1930.
(29) Galis, Z. S.; Sukhova, G. K.; Lark, M. W.; Libby, P. *J. Clin. Invest.* **1994**, *94*, 2493–2503.
(30) Samnegard, A. S., A.; Lundman, P.; Boquist, S.; Odeberg, J.; Hulthe, J.; McPheat, W.; Tornvall, P.; Bergstrand, L.; Ericsson, C. G.; Hamsten, A.; Eriksson, P. *J. Intern. Med.* **2005**, *258*, 411–419.
(31) Kaplan, R. C.; Smith, N. L.; Zucker, S.; Heckbert, S. R.; Rice, K.; Psaty, B. M. *Atherosclerosis* **2008**, *201*, 130–137.
(32) Kurzawski, M.; Modrzejewski, A.; Pawlik, A.; Drozdzik, M. *Clin. Exp. Dermatol.* **2009**, *34*, 613–617.
(33) Han, Z. N.; Boyle, D. L.; Manning, A. M.; Firestein, G. S. *Autoimmunity* **1998**, *28*, 197–208.
(34) Murawaki, Y.; Ikuta, Y.; Okamoto, K.; Koda, M.; Kawasaki, H. *J. Hepatol.* **1999**, *31*, 474–481.
(35) Gohji, K.; Fujimoto, N.; Komiyama, T.; Fujii, A.; Ohkawa, J.; Kamidono, S.; Nakajima, M. *Cancer* **1996**, *78*, 2379–2387.
(36) Lein, M.; Nowak, L.; Jung, K.; Koenig, F.; Schnorr, D.; Loening, S. A. *Urologe A* **1998**, *37*, 377–381.
(37) Preece, G.; Murphy, G.; Ager, A. *J. Biol. Chem.* **1996**, *271*, 11634–11640.
(38) Simian, M.; Hirai, Y.; Navre, M.; Werb, Z.; Lochter, A.; Bissell, M. J. *Development* **2001**, *128*, 3117–3131.
(39) Sternlicht, M. D.; Bissell, M. J.; Werb, Z. *Oncogene* **2000**, *19*, 1102–1113.
(40) Sternlicht, M. D.; Lochter, A.; Sympson, C. J.; Huey, B.; Rougler, J. P.; Gray, J. W.; Pinkel, D.; Bissell, M. J.; Werb, Z. *Cell* **1999**, *98*, 137–146.
(41) McCawley, L. J.; Wright, J.; LaFleur, B. J.; Crawford, H. C.; Matrisian, L. M. *Am. J. Pathol.* **2008**, *173*, 1528–1539.
(42) Si-Tayeb, K.; Monvoisin, A.; Mazzocco, C.; Lepreux, S.; Decossas, M.; Cubel, G.; Taras, D.; Blanc, J.-F.; Robinson, D. R.; Rosenbaum, J. *Am. J. Pathol.* **2006**, *169*, 1390–1401.
(43) Stevens, A. P.; Spangler, B.; Wallner, S.; Kreutz, M.; Dettmer, K.; Oefner, P. J.; Bosserhoff, A. K. *J. Cell. Biochem.* **2009**, *106*, 210–219.

EXPERIMENTAL SECTION

Preparation of 3-MPA-peptide-OH. Short thiolated binary patterned peptides were synthesized according to the procedure previously published for the synthesis of short homopeptides.[6] A minor difference is that the solid-phase synthesis support was replaced with a hydroxymethyl polystyrene resin. This precludes any change in the experimental conditions previously developed for hydroxymethylphenoxy polystyrene lanterns and allows a cost-effective and larger scale synthesis.[44] Numerous peptides, based on the general structure of 3-MPA-A_x-B_y-OH, where A is either Leu, Asp, His, or Ser and B is either Asp, His, or Ser, with $0 \leq x, y \leq 5$, and $x + y = 5$, were synthesized. LC-MS coupled with electrospray ionization validated the new approach and confirmed the mass of each final product. The overall yield varied between 15% and 70% depending on the peptide sequence. (See Supporting Information section for detailed procedure.)

Preparation and Characterization of Monolayers. Peptide-based SAMs were prepared overnight in DMF solutions as stated previously.[6,23] Monitoring of each SAM was accomplished on a Kretchmann SPR setup, based on a Dove prism.[45] Advancing contact angles with PBS were acquired with a home-built instrument. Peptide-based SAMs were also characterized using Ge-attenuated total reflection (ATR-FTIR). Quantification of nonspecifically adsorbed proteins on each surface was accomplished by exposing to PBS for baseline monitoring, followed by undiluted bovine serum and then PBS to monitor the baseline after nonspecific adsorption. (See Supporting Information section for detailed procedure.) CM-Dextran was prepared according to a previously reported procedure.[46,47]

Fabrication of SPR Biosensors and Detection of Biomolecules. IgG and MMP-3 specific biosensors were built using the EDC/NHS chemistry on the free carboxylic acid of the peptide.[48−51] Sensors fabricated as described above were mounted on the SPR instrument equipped with a fluidic cell, and the signal was stabilized for at least 5 min in 18 MΩ water. The solutions required for fabrication of a SPR affinity biosensor were sequentially injected to chemically derive the surface with an antibody monolayer, procuring the specificity to the SPR sensor. The measurement began with 2 min of reference in 18 MΩ water. Then, an aqueous solution composed of 100 mM *N*-ethyl-*N*′-(3-dimethylaminopropyl)-carbodiimide (EDC, Fluka) and 20 mM *N*-hydroxysuccinimide (NHS, Sigma-Aldrich) was injected for 2 min, followed by a rinsing step with PBS (pH 4.5) for 2 more min. A solution of 25 μg/mL antibody (anti-human IgG, Cedarlane laboratories Ltd., Burlington, ON, or anti-human MMP-3, GeneTex, Irvine, CA, according to the experiments described below) in PBS (pH 7.4) was injected for 15 min to derivatize the surface with antibody. The excess antibody was rinsed with PBS for 2 min before a 5-min exposition to a 1 M ethanolamine solution adjusted to pH 8.5. The SPR sensor was rinsed again for 5 min in PBS before injection of the analyte of interest. The detection assay was performed for 10 min with a PBS solution of IgG or MMP-3 (according to the antibody immobilized) and was followed by a 5-min baseline measurement in PBS.

Quantification of MMP-3 in Bovine Serum. The SPR biosensors were used for direct detection of biomolecules in serum and diluted serum. Biosensors were prepared as described above. In this experiment, a 2-min exposition to bovine serum verified occurrence of nonspecific interaction on these biosensors. Thereafter, bovine serum spiked with human MMP-3 to a concentration of 25 nM was injected on the SPR sensor. A blank serum measurement verified whether the SPR response monitored for MMP-3 was the result of specific interactions and not to nonspecific adsorption. As a further control, the spiked serum was diluted by a factor of 2 to 12.5 nM with PBS or with bovine serum to verify that the signal was proportional to the analyte concentration. Statistical analysis was performed to validate the response.

RESULTS AND DISCUSSION

Synthesis of Peptides. The peptide synthesis protocol was adapted from previous work based on SynPhase lanterns, to the hydroxymethyl polystyrene resin used here.[6] The modifications were necessary to reduce the production cost of the peptides with minimal optimization of the preparation steps. This approach allowed the production of the various peptides involved in this study. To confirm that the SynPhase lanterns protocol was valid for the hydroxymethyl polystyrene resin, the synthesis of a thiolated peptide was confirmed after each step using LC-MS. For example, prior to coupling of H_2N-HHHDD-OH with 3-MPA, the molecular ion was clearly visible at $m/z = 660.2$ indicating that the synthesis of the peptide was successful. The mass spectrum for the corresponding final product 3-MPA-HHHDD-OH showed a major signal at $m/z = 748.7$ corresponding to the expected mass molecular ion. It was revealed by LC-MS that significant fraction of the peptides formed disulfide bonds. For 3-MPA-HHHDD-OH, this was observed from a molecular ion at $m/z = 1494.5$; the final product adopted the disulfide form to a proportion of nearly 10%. It was also noticed that every product with His showed a yellow color in TFA, in accordance with prior observations for other His-containing peptidomimetic structures.[52] This color disappeared after complete evaporation of the solvent leaving a white to gray precipitate similar to other peptides. The overall synthetic yield varied from 15% to 70% depending on the sequence of the peptide.

Effect of Block Length in Binary Patterned Peptide SAMs. The combination of materials into hybrid materials yields properties that are not a linear combination of the properties of the individual materials. As an example, zwitterionic monolayers exhibit significantly decreased nonspecific adsorption.[53−55] This was observed for polymers of poly-L-lysine with poly styrene

(44) Roice, M.; Suma, G.; Kumar, K. S.; Pillai, V. N. R. *J. Protein Chem.* **2001**, *20*, 25–32.
(45) Bolduc, O. R.; Live, L. S.; Masson, J. F. *Talanta* **2009**, *77*, 1680–1687.
(46) Masson, J. F.; Battaglia, T. M.; Kim, Y. C.; Prakash, A.; Beaudoin, S.; Booksh, K. S. *Talanta* **2004**, *64*, 716–725.
(47) Masson, J. F.; Obando, L.; Beaudoin, S.; Booksh, K. *Talanta* **2004**, *62*, 865–870.
(48) Johnsson, B.; Löfås, S.; Lindquist, G. *Anal. Biochem.* **1991**, *198*, 268–277.
(49) Johnsson, B.; Löfås, S.; Lindquist, G.; Edström, Å.; Hillgren, R.-M. M.; Hansson, A. *J. Mol. Recognit.* **1995**, *8*, 125–131.
(50) Löfås, S.; Johnsson, B. *J. Chem. Soc., Chem. Commun.* **1990**, 1526–1528.
(51) Löfås, S.; Johnsson, B.; Tegendal, K.; Rönnberg, I. *Colloids Surf., B.* **1993**, *1*, 83–89.
(52) Simone, Z.; Roger, S.; Esther, Y. *Eur. J. Org. Chem.* **2003**, *2003*, 2454–2461.
(53) Chang, Y.; Chen, S. F.; Zhang, Z.; Jiang, S. Y. *Langmuir* **2006**, *22*, 2222–2226.
(54) Yang, W.; Xue, H.; Li, W.; Zhang, J. L.; Jiang, S. Y. *Langmuir* **2009**, *25*, 11911–11916.
(55) Yang, W.; Zhang, L.; Wang, S. L.; White, A. D.; Jiang, S. Y. *Biomaterials* **2009**, *30*, 5617–5621.

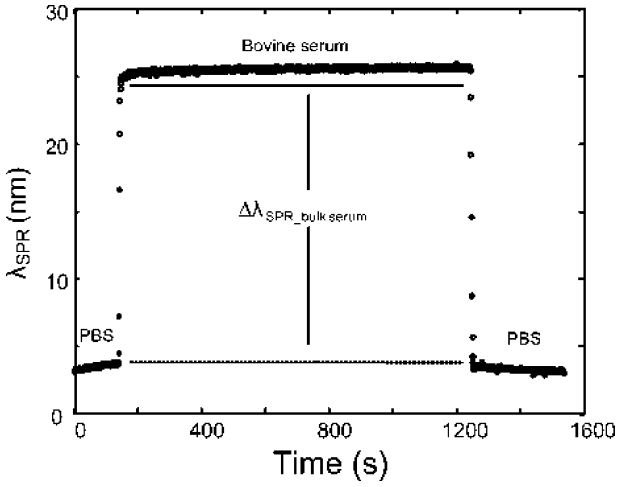

Figure 1. Sensorgram demonstrating low nonspecific adsorption of bovine serum proteins on a SAM of 3-MPA-HHHDD-OH.

sulfonate,[56] where a mixed copolymer significantly decreased nonspecific adsorption. This approach is investigated here with block peptides, peptides constituted of a block of one amino acid at the N-terminus and a block of another amino acid at the C-terminus, exposed to the solution. In a first study, the optimal composition of the block length for a binary patterned pentapeptide was determined with a series of peptides with the general composition 3-MPA-H_x-D_y-OH, where $0 \leq x, y \leq 5$, and $x + y = 5$. The optimal length of peptide monolayer was previously determined to be five residues long for maximal reduction of nonspecific interactions;[6] hence all peptides in this study are of that length. The peptides were synthesized with His at the N-terminus (in the base) to leave the Asp block, rich in COOH, surface-exposed for later reaction in immobilizing molecular receptors. Each block was varied from 0 to 5 to investigate all possible combinations of a His/Asp diblock pentapeptide.

Nonspecific adsorption of proteins contained in biological media has greatly limited the use of many biosensors by producing a false positive response. Therefore, measuring the nonspecific adsorption of binary patterned peptides on Au surfaces is essential in assessing the potential of these monolayers in biosensing templates. The surface coverage for nonspecific adsorption of proteins on binary patterned peptide SAMs was obtained from the equations of Jung et al.[57,58] and the parameters previously published.[6] Figure 1 shows a sensorgram obtained for 3-MPA-HHHDD-OH. A 5 min period in PBS allowed the system to stabilize before PBS was replaced with bovine serum containing 76 mg/mL of proteins. The protein concentration in bovine serum is similar to human serum making this model relevant. An important portion of the shift of signal observed during this replacement was due to the bulk change of refractive index between PBS and serum. The SPR response to nonspecific adsorption was obtained at least four times for every peptide.

Nonspecific adsorption was greatly decreased using binary patterned peptides (Figure 2, left panel). Homopeptides 3-MPA-HHHHH-OH and 3-MPA-DDDDD-OH showed relatively high nonspecific adsorption at nearly 200−300 ng/cm^2. However, binary patterned peptides with these same two amino acids arranged in blocks decreased nonspecific interaction by 1 order of magnitude. Nonspecific adsorption of serum decreased for peptides with increasing block length of either of the two different amino acids. Nonspecific adsorption decreased to a minimum (32 ng/cm^2) for a peptide with the composition 3-MPA-HHHDD-OH. This is significantly lower than PEG, which exhibits approximately 100 ng/cm^2 of nonspecific adsorption,[6] and CM-Dextran (829 ± 46 ng/cm^2) using an identical experimental setup and solutions. This signifies that binary patterned peptides significantly improve nonspecific adsorption compared to the homopeptides and to state-of-the-art PEG. Similarly, a decrease of 1 order of magnitude for mixed monolayers compared to pure components has been observed with poly-L-lysine and poly styrene sulfonate.[56] To extend these results to a variety of peptide compositions, further binary patterned peptides with the same 3-MPA-AAABB-OH configuration were also investigated (vide infra).

Characterization of the Peptides with Contact Angle, Mid-IR, Circular Dichroism, and Capillary Electrophoresis. To better understand the physicochemical effects involved in the decrease of the nonspecific adsorption to these binary patterned peptide surfaces, several studies were undertaken. Contact angle measurements are related to the hydrophilicity of the monolayers. In the case of binary patterned peptides, contact angle increased upon combining blocks of Asp and His to reach a maximum plateau of approximately 35° for 3-MPA-HHDDD-OH, 3-MPA-HHHDD-OH, and 3-MPA-HHHHD-OH (Figure 2, right panel), roughly correlating with decreased nonspecific adsorption. Highly charged surfaces (e.g., CM-dextran) were previously found to increase nonspecific adsorption.[5] Hence, it is possible that the decrease of nonspecific adsorption is related to the zwitterionic character of these binary patterned peptides, as observed with several polymers.[26,56] To verify if this difference in nonspecific adsorption is caused by the global charge of the peptide, capillary electrophoresis was accomplished for the peptides providing the greatest decrease in nonspecific adsorption. Calibration runs were accomplished demonstrating that the difference in global charge between 3-MPA-HHDDD-OH, 3-MPA-HHHDD-OH, and 3-MPA-HHHHD-OH was almost negligible. Their global charge was approximately −1 as determined by capillary electrophoresis, indicating that the peptides carry one more carboxylate anion than iminium cation. Hence, it appears that the binary patterned peptide surfaces with lowest nonspecific adsorption exhibit a strong zwitterionic character.

Peptides in solution exhibit structures which are essential for their biological functions. However, it is well-known that antibodies are denatured to some extent when immobilized directly on Au. It was thus of interest to observe whether the peptide monolayer on the Au surface adopted any significant secondary structure, to provide insight on the potential formation of a "biologically compatible monolayer". The secondary structure of peptides on a surface is generally monitored via the amide I and II bands visible by mid-IR (Figure 3).[59] Peptides adopting an α-helical configuration show a strong amide I band at 1645 cm^{-1}, while

(56) Kurita, R.; Hirata, Y.; Yabuki, S.; Yokota, Y.; Kato, D.; Sato, Y.; Mizutani, F.; Niwa, O. *Sensors Actuators, B* **2008**, *130*, 320–325.
(57) Jung, L. S.; Campbell, C. T.; Chinowsky, T. M.; Mar, M. N.; Yee, S. S. *Langmuir* **1998**, *14*, 5636–5648.
(58) Nordin, H.; Jungnelius, M.; Karlsson, R.; Karlsson, O. P. *Anal. Biochem.* **2005**, *340*, 359–368.
(59) Sakurai, T.; Oka, S.; Kubo, A.; Nishiyama, K.; Taniguchi, I. *J. Pept. Sci.* **2006**, *12*, 396–402.

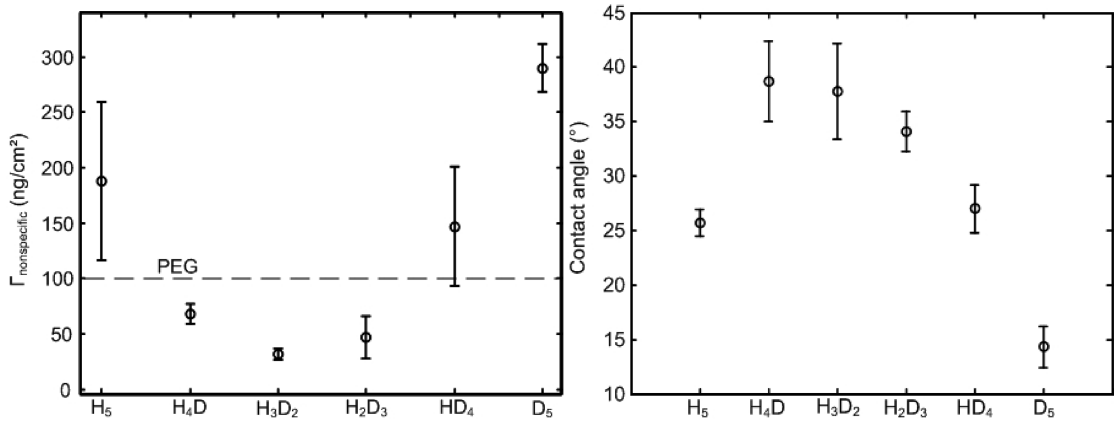

Figure 2. (Left) Reduction of nonspecific adsorption with binary patterned peptides. (Right) Contact angle with binary patterned peptides. The peptides are identified as: H_5 for 3-MPA-HHHHH-OH, H_4D for 3-MPA-HHHHD-OH, H_3D_2 for 3-MPA-HHHDD-OH, H_2D_3 for 3-MPA-HHDDD-OH, HD_4 for 3-MPA-HDDDD-OH, and D_5 for 3-MPA-DDDDD-OH. The error bars represent two standard deviations of the mean.

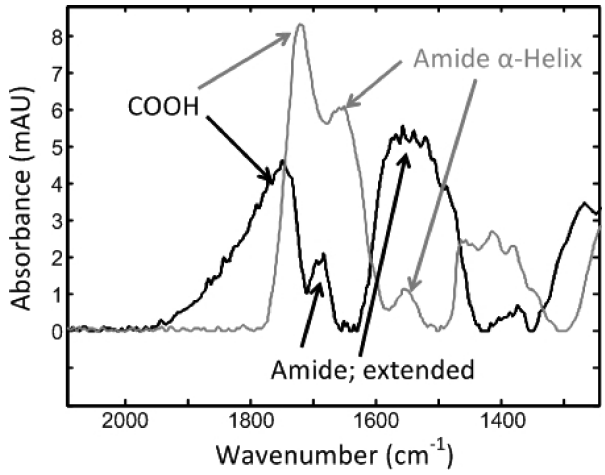

Figure 3. Determination of the extended or α-helix configuration of a binary patterned peptide SAM using FT-IR. The gray line is for 3-MPA-LLLDD-OH and is representative of the signal observed for all other binary patterned peptides except for 3-MPA-HHHDD-OH which is represented by the black line.

peptides autoassembling in the extended configuration lead to a shifted amide I at 1675 cm^{-1}.[59,60] Interestingly, all peptides investigated here adopted an α-helical configuration except for 3-MPA-HHHDD-OH. These results indicate that the peptides adopt a secondary structure on the surface and are not "quenched" by the Au surface. The conformation of 3-MPA-HHHDD-OH and 3-MPA-LLLDD-OH was also assessed in PBS using circular dichroism. In accordance with mid-IR results, 3-MPA-HHHDD-OH adopted an extended conformation in PBS, while 3-MPA-LLLDD-OH exhibited an α-helical conformation. The interpretation of circular dichroism data was performed according to Doneux et al.[61] However, the high performance of 3-MPA-HHHDD-OH in decreasing nonspecific adsorption cannot be correlated with adoption of the extended configuration, as other peptides exhibited similar nonspecific adsorption while adopting an α-helical configuration.

Effect of the Physicochemical Properties of the Different Blocks in Binary Patterned Peptides. To test if a further decrease in nonspecific adsorption could be obtained with binary patterned peptides, every possible combination of the form 3-MPA-AAABB-OH was synthesized, where A is either His, Asp, Ser, or Leu and B is His, Asp, or Ser. The resulting peptides tested the four major physicochemical properties for the N-terminal block: hydrophobic (Leu), polar (Ser), acidic (Asp), and basic (His), where Leu was introduced to investigate the influence of a hydrophobic block on nonspecific interactions in complex biological matrixes. The C-terminal block was always constituted of hydrophilic residues, either neutral or charged. By those means, generalities on the influence of the peptide physicochemical properties could be observed.

Table 1. Characterization of Block Peptide SAMs Immobilized on the Gold Surface of a SPR Biosensor[a]

sequence	$\Delta\Gamma_{nonspecific}$ (ng/cm²)
3-MPA-SSSDD-OH	23 ± 10
3-MPA-HHHDD-OH	32 ± 5
3-MPA-LLLDD-OH	35 ± 23
3-MPA-LLLSS-OH	39 ± 13
3-MPA-LLLHH-OH	45 ± 11
3-MPA-HHHSS-OH	48 ± 18
3-MPA-DDDHH-OH	56 ± 22
3-MPA-DDDSS-OH	69 ± 40
3-MPA-SSSHH-OH	79 ± 50

[a] The error represents two standard deviations.

The different peptide monolayers were classified from the most to the least resistant to nonspecific adsorption of serum proteins (Table 1), highlighting the relationship between the peptide sequence and their performance in limiting nonspecific adsorption. Two distinct trends were observed. First, the three monolayers displaying the least nonspecific interactions with bovine serum had Asp as the C-terminal block. These monolayers present the dual advantage of improved resistance to nonspecific interactions and potentially improving bioreagent immobilization, since the free carboxylates should be available for attachment of a recognition molecule (antibody, enzyme, DNA, aptamer or others) through NHS-ester chemistry. While 3-MPA-SSSDD-OH offered slightly better performance, its synthetic yield was four times lower than 3-MPA-HHHDD-OH, hindering its use in practical applications. This led to the selection of 3-MPA-HHHDD-OH for subsequent experiments.

(60) Duevel, R. V.; Corn, R. M. *Anal. Chem.* **1992**, *64*, 337–342.

(61) Doneux, T.; Bouffier, L.; Mello, L. V.; Rigden, D. J.; Kejnovska, I.; Fernig, D. G.; Higgins, S. J.; Nichols, R. J. *J. Phys. Chem. C* **2009**, *113*, 6792–6799.

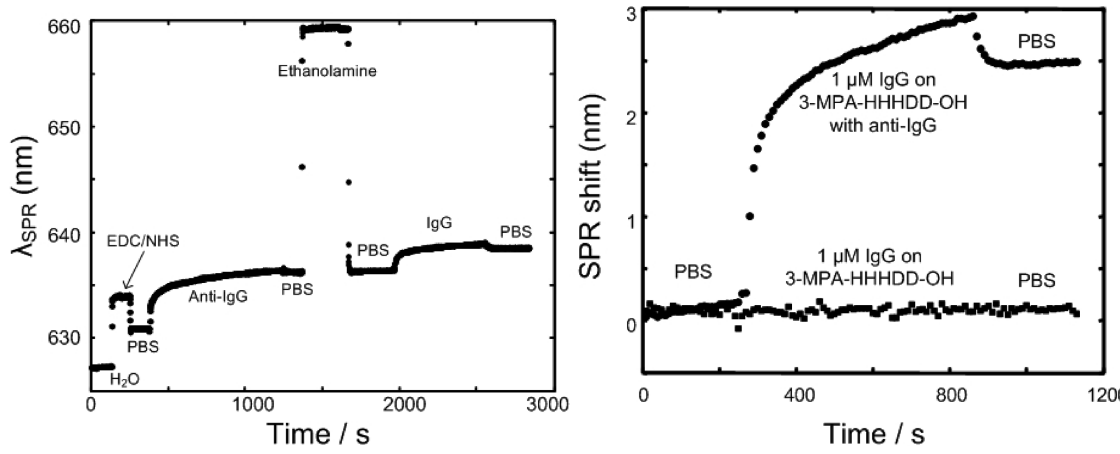

Figure 4. (Left) Sensorgram for the fabrication of an IgG specific biosensor. This SPR sensor held a 3-MPA-HHHDD-OH monolayer. (Right) Detection of 1 μM IgG on a 3-MPA-HHHDD-OH sensor reacted with anti-IgG (positive control) and response to the same solution of a sensor with 3-MPA-HHHDD-OH (negative control).

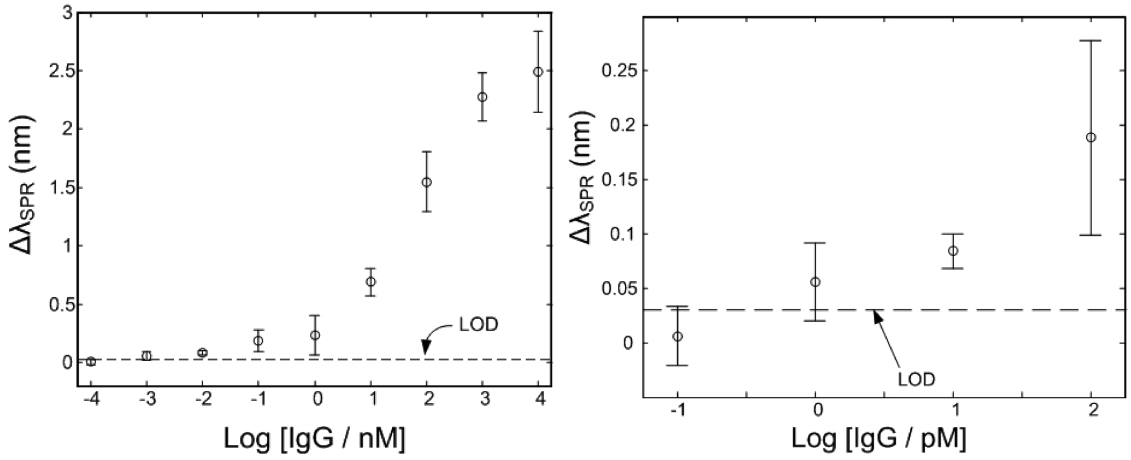

Figure 5. (Left) Calibration curve of IgG in PBS. The concentration of IgG is given in a logarithmic scale in nM. (Right) Low-sensitivity response of IgG in the pM range, with a LOD of 3 pM. The error bars represent two standard deviations of the mean.

Interestingly, each binary patterned peptide maintained excellent resistance to nonspecific adsorption, where adsorption of nonspecific proteins ranged from 23 to 79 ng/cm^2 (Table 1). These values are extremely low, as the resistance to nonspecific interactions from bovine serum typically ranges between 100 to 1000 ng/cm^2.[5,23,62,63] Specifically, these values are inferior by roughly 1 order of magnitude with most monolayers and by up to a factor of 4 compared to state-of-the-art PEG monolayers.[6] Also providing low nonspecific adsorption, monolayers including a Leu base offered the third to fifth best performances among the binary patterned peptides tested. These results show that a zwitterionic monolayer is not essential for ultralow fouling. It suggests that the combination of different physicochemical properties within a single monolayer such as charge for zwitterionic monolayers or hydrophobicity/hydrophilicity in others is a condition for ultralow fouling. As we demonstrate below, this improvement allowed direct detection assays in complex matrixes.

SPR Biosensors with Binary Patterned Peptide SAMs: 3-MPA-HHHDD-OH. To demonstrate the efficiency of binary patterned peptide SAMs to immobilize biorecognition molecules, such as antibodies, in the construction of an affinity biosensor, an IgG biosensor was demonstrated. IgG detection is commonplace in biosensing and provides an excellent comparison point with other techniques and approaches. To fabricate this biosensor, a series of chemical reactions were performed on the binary patterned peptide monolayer, as demonstrated in Figure 4 (left panel). The interaction between IgG and anti-IgG is strong, as observed from the slow return to the initial baseline during the last exposition to PBS of the IgG biosensor (longer than the data acquisition). This is expected as IgG and anti-IgG has a large binding constant. Hence, the 3-MPA-HHHDD-OH is suitable for biosensor construction. A control was performed with the unreacted 3-MPA-HHHDD-OH surface. One μM IgG was injected on the sensor, which showed no response to IgG, unless the antibody was immobilized to the peptide monolayer (positive control).

The calibration curve of IgG, using a SPR sensor derived with 3-MPA-HHHDD-OH and anti-IgG, showed the expected behavior of a Langmuir isotherm (Figure 5, left). The binding constant of IgG/anti-IgG measured on peptide monolayer is 2.6×10^7 M^{-1}. This is consistent with the anti-IgG/IgG affinity constant published elsewhere, which was as high as 3.2×10^7 M^{-1}.[64] A linear domain of SPR response was observed within the nM concentration range

(62) Bolduc, O. R.; Clouthier, C. M.; Pelletier, J. N.; Masson, J. F. *Anal. Chem.* **2009**, *81*, 6779–6788.

(63) Masson, J. F.; Battaglia, T. M.; Cramer, J.; Beaudoin, S.; Sierks, M.; Booksh, K. S. *Anal. Bioanal. Chem.* **2006**, *386*, 1951–1959.

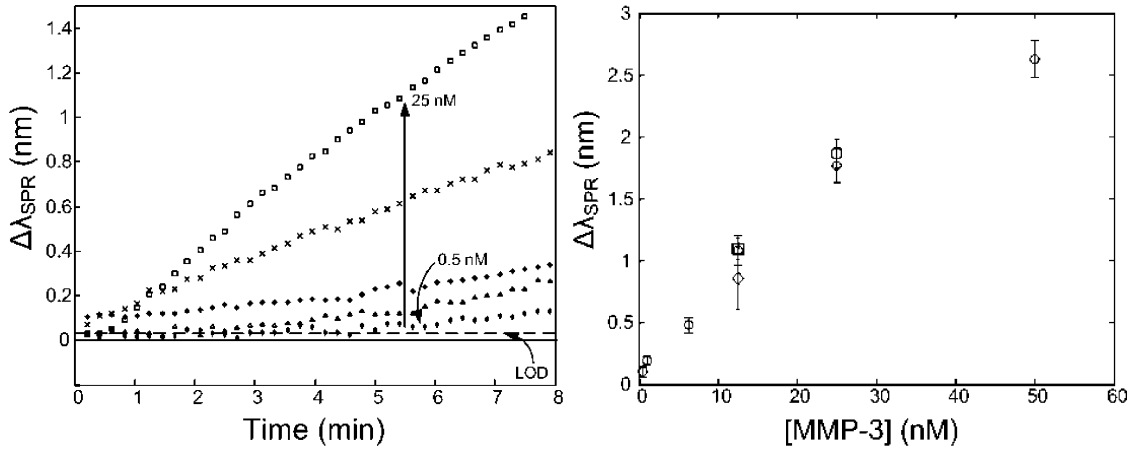

Figure 6. (Left) Overlay of sensorgrams for the detection of different concentrations of MMP-3 in PBS. The concentrations detected are 0.5, 1, 6, 12.5, and 25 nM. (Right) Calibration curve of MMP-3 in PBS (○, $n = 3$; number of replicate measurements at each concentration). Quantification of MMP-3 in complex matrixes: □ shows the detection of 12.5 and 25 nM MMP-3 in full bovine serum; ◇ shows the detection of 12.5 nM MMP-3 in 1:1 bovine serum/PBS. The error bars represent two standard deviations of the mean.

Scheme 1. Schematic Structure of the Peptide Monolayers on the Au Surface, as a Native Peptide (Top), a Peptide Activated with NHS (Middle), and with the Antibody Cross-Linked to the Peptide (Bottom)

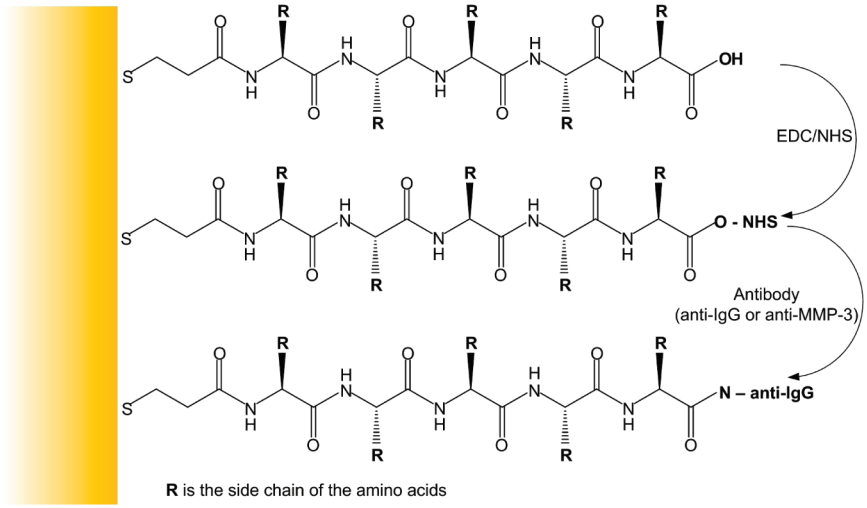

(from 0 to 3 in the logarithmic concentration scale). This domain delimits the concentration of interest that could be determined with high sensitivity using this SPR biosensor. The SPR response observed outside this domain was saturated at higher concentrations and exhibited low sensitivity at lower concentrations. An apparent detection limit of 0.11 nM was obtained from this high sensitivity domain, which is typically used for the determination of LOD in SPR. This LOD is calculated with 3 times the noise on the SPR sensorgram ($3\sigma = 0.03$ nm), with the slope of the highly sensitive region. Among others, SPR imaging sensors exhibited a detection limit of 3.7 nM for direct detection of IgG.[64] In our work, the lower LOD by 1 order of magnitude is explained by the wavelength interrogation method being more accurate than the intensity measurement.[1] However, the low-sensitivity region of the calibration curve still exhibited a response proportional to concentration and greater than the limit of detection. We conclude that the actual limit of detection for IgG would be between 1−10 pM, similar or better than that reported for other biosensors. Because of the low sensitivity of this region, an exact LOD is not reported. Lower detection limits have been obtained with sandwich immunoassays using SERS (19 pM),[65] SPR (6.7 pM),[66] chemiluminescence (3 pM),[67] anodic stripping voltammetry (3 pM),[68] and LSPR with Ag nanoparticles (9 pM).[69] However, these methods require multistep detection schemes.

Calibration of MMP-3 in PBS. The possibility of substituting antibodies for other biologically relevant problems is an important advantage of SPR biosensors. MMP-3 is an important biomarker to monitor various diseases. Hence, a SPR sensor was prepared as for IgG, with the exception of anti-human MMP-3 acting as the recognition biomolecule for human MMP-3. The sensorgrams for different concentrations of MMP-3 showed increasing intensity of the SPR responses to increasing concentration of MMP-3 in PBS (Figure 6, left). The correlation coefficient (R^2) for this calibration curve is 0.96 indicating a strong linear relationship

(64) Dong, Y.; Wilkop, T.; Xu, D. K.; Wang, Z. Z.; Cheng, Q. *Anal. Bioanal. Chem.* **2008**, *390*, 1575–1583.

(65) Ni, J.; Lipert, R. J.; Dawson, G. B.; Porter, M. D. *Anal. Chem.* **1999**, *71*, 4903–4908.

(66) Lyon, L. A.; Musick, M. D.; Natan, M. *J. Anal. Chem.* **1998**, *70*, 5177–5183.

(67) Fan, A. P.; Lau, C. W.; Lu, J. Z. *Anal. Chem.* **2005**, *77*, 3238–3242.

(68) Dequaire, M.; Degrand, C.; Limoges, B. *Anal. Chem.* **2000**, *72*, 5521–5528.

(69) Ling, J.; Li, Y. F.; Huang, C. Z. *Anal. Chem.* **2009**, *81*, 1707–1714.

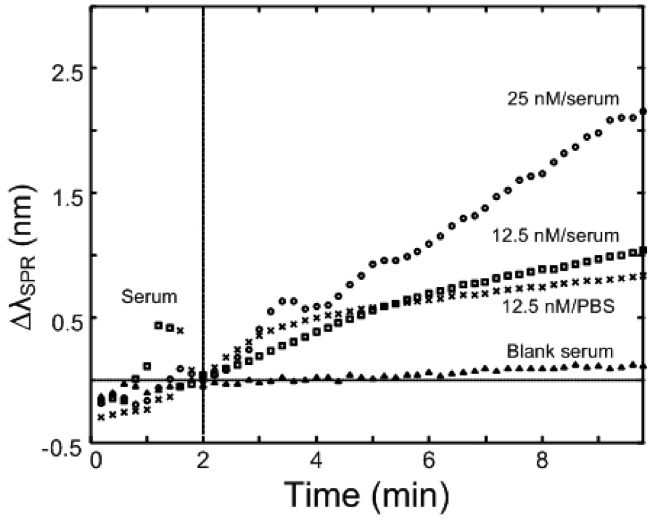

Figure 7. Detection of human MMP-3 in complex matrixes. The baseline was monitored in serum for 2 min before injecting serum spiked with MMP-3. MMP-3 was spiked into bovine serum (exempt of human MMP-3) at 25 nM (○). A 1:1 dilution with bovine serum (□) and with PBS (×), decreased this concentration to 12.5 nM. The blank (Δ) demonstrates that the SPR response observed for the three other sensorgrams is due to specific interactions of MMP-3 with anti-MMP-3.

between the SPR response from MMP-3 and the concentration of MMP-3. The slight deviation from unity of the regression coefficient could be explained by the nonlinearity at high concentration of the Langmuir isotherm. The calibration allows the quantification of MMP-3 over a targeted domain of concentrations comprised between 0.5 and 50 nM, with a detection limit at 0.14 nM. Moreover, addition of PBS led to a nearly complete return of the SPR response to initial value prior to MMP-3 binding (data not shown), suggesting that MMP-3 binding to anti-MMP-3 was rapidly reversible.

Detection and Quantification of MMP-3 in Bovine Serum. To demonstrate the efficiency of 3-MPA-HHHDD-OH in reducing the level of nonspecific interactions with the surface of a biosensor, detection of MMP-3 was performed in undiluted bovine serum. The two-minute pre-exposition of the SPR sensor to serum exempt of MMP-3 showed little response resulting from nonspecific interactions (Figure 7). This further demonstrates that the peptide-derived SPR biosensor is very stable in undiluted serum. Figure 7 shows the SPR response of 25 nM MMP-3 in serum, which was significantly different than the response of a blank serum sample. As highlighted in Figure 6, the detection of 25 nM MMP-3 in bovine serum resulted in a SPR response statistically identical to the detection of 25 nM MMP-3 in PBS. The predicted concentration for the detection of 25 nM in PBS using the linear calibration model in PBS results is 30 ± 2 nM. The deviation between the predicted and actual concentration is the result of the slight deviations from linearity observed with the Langmuir model. Detecting the same concentration in undiluted serum resulted in a predicted concentration of 32 ± 2 nM. This indicates that the serum does not influence the detection of MMP-3 in a complex biological matrix and that the response is identical to the one measured in saline solution.

Dilution of the MMP-3 serum sample with serum or PBS provided a comparative study to evaluate the influence of serum on the detection of MMP-3 in complex matrixes. The dilution of MMP-3 to 12.5 nM with PBS or serum resulted in a proportional decrease of the SPR response (Figure 7). The similar SPR response with 12.5 nM MMP-3 in serum (predicted concentration of 17 ± 1 nM) and 1:1 PBS/serum (predicted concentration of 12 ± 4 nM) suggests that nonspecific protein adsorption in undiluted serum has a minimal influence on the measured SPR response. This is very similar to the predicted concentration of 12.5 nM MMP-3 measured in PBS (predicted concentration of 17 ± 2 nM). These assays demonstrated the efficacy of binary patterned peptide SAMs immobilized on the SPR biosensors for detection assays in complex analytical matrixes. Lastly, a direct detection assay, without flowing blank bulk bovine serum over the biosensor before injecting the serum containing 25 nM of MMP-3, led to similar results although the shift observed was overestimated by 15% due to previously observed minimal nonspecific adsorption still taking place. This could easily be taken into account in calibration models. Therefore, binary patterned peptide monolayers are suitable for detection of low nM levels of MMP-3 in serum, without sample pretreatment or signal amplification.

CONCLUSION

This article demonstrates the efficacy of binary patterned peptide self-assembled monolayers (SAMs) to reduce nonspecific interactions caused by bulk proteins in complex analytical matrixes to a level allowing the quantification of a biological molecule of clinical interest in undiluted serum. Various studies revealed that the decrease in nonspecific adsorption provided by binary patterned peptides or other ultralow fouling monolayers is unrestricted to the zwitterionic character and also includes monolayers combining mixed physicochemical properties. Various peptide compositions, including 3-MPA-HHHDD-OH, exhibited ultralow fouling properties. The calibration of IgG using SPR biosensors, based on the binary patterned peptide 3-MPA-HHHDD-OH, verified the potential of such SAMs for building SPR biosensors, with an excellent detection limit of 1−10 pM. MMP-3, an upregulated marker in cancer, was quantified by applying the same protocol leading to a quantification of low nanomolar amount of this analyte in undiluted bovine serum. The detection limit for the MMP-3 biosensor was 0.14 nM. These two examples of biosensing with binary patterned peptide monolayers demonstrate the strong potential of this methodology for SPR sensors.

ACKNOWLEDGMENT

The authors would like to thank William D. Lubell and Caroline Proulx from Université de Montréal, for technical assistance in synthesizing the peptides. Financial support was provided by NanoQuébec, the Canadian Space Agency, the Canada Foundation for Innovation (CFI), the National Sciences and Engineering Research Council of Canada (NSERC), the Fonds Québécois de la Recherche sur la Nature et les Technologies (FQRNT).

SUPPORTING INFORMATION AVAILABLE

Additional information as noted in the text. This material is available free of charge via the Internet at http://pubs.acs.org.

Received for review January 6, 2010. Accepted March 18, 2010.

AC100035S